SSCL-Preprint-491

SSCL-Preprint-491
July 1993
Distribution Category: 414

B. Abbott, et al.

Beam Test of a 12-layer Scintillating Fiber Charged Particle Tracking System

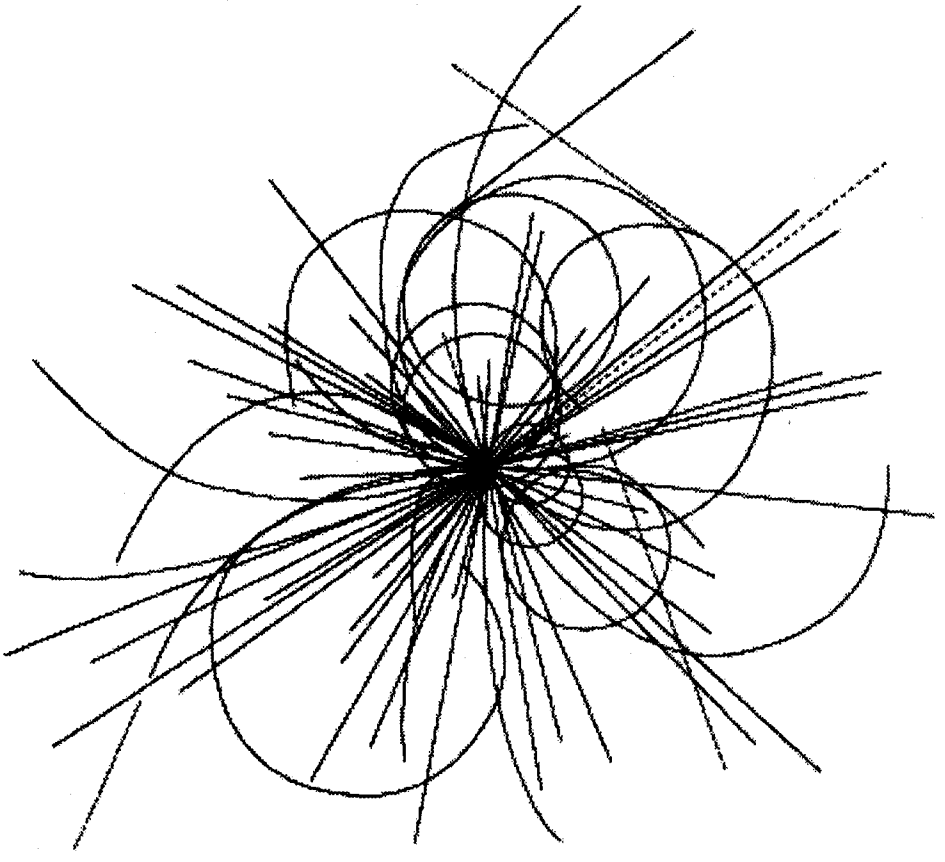

Superconducting Super Collider Laboratory

SSCL-Preprint-491

Beam Test of a 12-layer Scintillating Fiber Charged Particle Tracking System*

B. Abbott, B. Howell, d. Koltick, R. McIlwain, C. Schmitz, E. Shibata, and Z. Zhou
Department of Physics, Purdue University
West Lafayette, IN 47907, USA

B. Baumbaugh, M. Ivancic, J. Jaques, R. Kehoe, M. Kelley, Q. Lu, M. Mahoney, R. Ruchti, and M. Wayne
Department of Physics, University of Notre Dame
Notre Dame, IN 46556, USA

S. Margulies and J. Solomon
Department of Physics, University of Illinois at Chicago
Chicago, IL 60680, USA

R. Chaney and J. Orgeron
Department of Physics, University of Texas at Dallas
Richardson, TX 75083, USA

A. Baumbaugh, J. Elias, and A. Romero
Fermi Laboratory
P.O. Box 500, Batavia, IL 60510, USA

T. Armstrong, R. Lewis, G. Mitchell, R. Moore, J. Passaneau, and G. Smith
Department of Physics, Pennsylvania State University
University Park, PA 16802, USA

M. Corcoran and D. Adams
Department of Physics, Rice University
Houston, TX 77251, USA

F. Bird, H. Fenker, T. Regan, and J. Thomas
Superconducting Super Collider Laboratory†
2550 Beckleymeade Ave.
Dallas, TX 75237

July, 1993

*Submitted to the "Nuclear Instruments and Methods in Physics Research".
†Operated by the Universities Research Association, Inc., for the U.S. Department of Energy under Contract No. DE-AC35-89ER40486.

SDC-93-514
D0 note #1729

Beam Test of a 12-layer Scintillating Fiber Charged Particle Tracking System

Scintillating Fiber Tracking Group

B. Abbott, B. L. Howell, D. Koltick, R. L. McIlwain,
C. J. Schmitz, E. I. Shibata, and Z. Zhou
Department of Physics, Purdue University, West Lafayette, IN 47907, USA

B. Baumbaugh, M. Ivancic, J. Jaques, R. Kehoe, M. Kelley,
Q. Lu, M. Mahoney, R. Ruchti, and M. Wayne
Department of Physics, University of Notre Dame, Notre Dame, IN 46556, USA

S. Margulies and J. Solomon
Department of Physics, University of Illinois at Chicago, Chicago, IL 60680, USA

R. Chaney and J. Orgeron
Department of Physics, University of Texas at Dallas, Richardson, TX 75083, USA

A. Baumbaugh, J. E. Elias, and A. Romero
Fermilab, P. O. Box 500, Batavia, IL 60510, USA

T. Armstrong, R. A. Lewis, G. S. Mitchell, R. S. Moore,
J. Passaneau, and G. S. Smith
Department of Physics, Pennsylvania State University, University Park, PA 16802, USA

M. Corcoran and D. Adams
Department of Physics, Rice University, Houston, TX 77251, USA

F. Bird, H. Fenker, T. Regan, and J. Thomas
Superconducting Super Collider Laboratory, Dallas, TX 75237, USA

Abstract

A 96-channel, 3-superlayer scintillating fiber tracking system has been tested in a 5 GeV/c π^- beam. The scintillating fibers were 830 μm in diameter, spaced 850 μm apart, and 4.3 m in length. They were coupled to 6 m long clear waveguides and finally to Visible Light Photon Counters. A spatial resolution of $\sim$ 150 μm for a double-layered ribbon was achieved with this tracking system. This first prototype of a charged particle tracking system configured for the Solenoidal Detector Collaboration at the Superconducting Super Collider was a benchmark in verifying the expected number of photoelectrons from the fibers.

1. Introduction

A scintillating fiber is an optical fiber with a doped core and one or more claddings. Its core emits light upon the passage of a charged particle. A fraction of the light (3 to 4%) is captured in the fiber and propagates through a clear waveguide to a photodetector. The instrumentation of a single scintillating fiber is shown in Figure 1. A system of many fibers in known locations can be used to track charged particles.

The optimal photodetector for this system is the Visible Light Photon Counter[1] (VLPC), a solid state device which has high quantum efficiency (55 to 85%), moderate gain ($\sim 2 \times 10^4$), and a fast time response ($\sim$ 5 ns). However, VLPCs must be operated at low temperature (6–10 K).

A scintillating fiber tracking system has many attractive features:

1. Good spatial resolution as a result of the small scintillating fiber diameter. The double-layered ribbons discussed in this paper have achieved spatial resolutions $\sigma \sim$ 150 μm.
2. Low occupancies as the result of small diameter ($\sim$ 1 mm) scintillating fibers and fast time response of the scintillating fluors and VLPCs.
3. Binary (yes/no) readout, thus simplifying electronics.
4. Insensitivity to magnetic fields and to radio-frequency noise.
5. No power dissipation within the tracking volume.
6. Participation of scintillating fibers in the first level trigger of an experiment. For example, the fast time response and small diameters of the fibers can be exploited to give an adjustable transverse momentum threshold with a sharp turn-on.
7. Radiation-hard elements. The fibers are radiation-hard to $\geq$ 10 Mrad for for light of wavelength $\lambda > 500$ nm and the VLPCs to $\geq$ 100 krad.

These features make scintillating fibers an excellent technology for charged particle tracking in experiments at the high energy, high luminosity hadron-hadron colliding beam machines in operation (e.g., the Fermilab Tevatron) or planned for the future. In particular, they are

well-suited for the Superconducting Super Collider (SSC) and the Large Hadron Collider (LHC) experiments, such as the one proposed by the Solenoidal Detector Collaboration (SDC)[2] at the SSC. The SSC and LHC have design luminosities $\mathcal{L} \geq 10^{33}$ cm^{-2}s^{-1} and beam crossings every 16 to 20 ns. Combined with the large pp total cross section ($\sim$ 100 mb) and high particle multiplicities ($\sim$ 100 per event), the demands on a tracking system are severe. Radiation-hard scintillating fibers of small diameter ($\leq$ 1 mm) can satisfy the requirements for a charged particle tracking system in such an environment.

2. Apparatus

2.1 Layout of the Experiment

A system of 96 fibers was tested in the A-2 external beam line of the Brookhaven National Laboratory Alternating Gradient Synchrotron. The fibers were arranged in three superlayers, which were each made of four layers of scintillating fibers. Figure 2 shows the arrangement of the system in the beam. To minimize multiple scattering effects, the beam momentum was set for negatively charged particles at the highest nominal value of 5 GeV/c. For our purposes the beam was defined by three small scintillation counters S1, S2, and S3 placed in coincidence to trigger the readout of the system. The three superlayers could be moved as a unit parallel to the axis of the fibers in order to take data from various locations along the fiber length. The typical flux was 2000 π^- per 1 second spill.

2.2 Scintillating Fibers

The scintillating fibers consisted of a polystyrene core doped with scintillation dyes and clad with a thin ($\sim$ 30 μm in thickness) layer of polymethylmethacrylate (PMMA). The primary scintillating fluor was p-terphenyl (PTP) at a concentration of 1% by weight, and the secondary fluor was 3-hyroxyflavone (3HF) at a concentration of 0.1% by weight.[3] This combination has fluorescence emission peaked near wavelength $\lambda \approx 530$ μm. This wavelength is desirable because (1) general optical transmission is best in unirradiated polystyrene for wavelengths 500 nm $< \lambda <$ 650 nm, and (2) the effects of radiation damage on optical transmission in polystyrene are substantially reduced[4] for $\lambda >$ 500 nm. Each of the tested scintillating fibers had a nominal diameter of 830 μm and was 4.3 m long.

Double-layered scintillating fiber ribbons (doublets) are the fundamental building blocks of our tracking system. For large scale scintillating fiber tracking systems, fiber-by-fiber placement and instrumentation is impractical. Precisely made ribbons of many fibers facilitate construction and can greatly reduce the number of spatial calibration constants. Furthermore, if ribbons can be layered with precise offsets with respect to the first layer, the spatial resolution can be enhanced with respect to ribbons layered with random offsets. An N-layered ribbon of fibers with center-to-center spacing D with each layer offset

by D/N has a theoretical spatial resolution given by

$$\sigma \leq \frac{D}{N\sqrt{12}}. \tag{1}$$

In comparison, the spatial resolution of a an N-layer system with random offsets is given by

$$\sigma = \frac{D}{\sqrt{12N}}. \tag{2}$$

For the doublets used in this beam test, equation (1) gives a doublet resolution of $\sigma = 123\ \mu$m, which is comparable to the spatial resolution obtained by typical large drift chambers.

The probability that a charged particle passes through a doublet without detection is small. For example, if a particle passes through the small gap between fibers in one layer, it will encounter the full diameter of a fiber in the other layer for which there is high detection efficiency.

Doublets of scintillating fibers were made by laying down a single layer of fibers on a precisely grooved aluminum jig plate to maintain a nominal 850 μm spacing between individual fibers, and then placing a second layer of fibers in the natural grooves of the first layer. The doublet ribbon was then painted with a water-based glue[5] and left to dry for about twelve hours.

Due to the possibility of damage[6] to the 3-HF by exposure to light with $\lambda < 500\ \mu$m, the scintillating fibers were handled in filtered light with $\lambda > 500\ \mu$m. The registration of individual fibers with respect to the nominal 850 μm spacing has been measured to have $\sigma < 20\ \mu$m with this manufacturing method.

2.3 Superlayers

As shown in Figure 3, doublets were glued to each side of a 1.6 cm thick carbon fiber composition board[7] to form a superlayer. Each side of a board was made of two layers of 0.18 mm thick composite carbon fiber-epoxy prepreg bonded to a rohacell[8] core to form a rigid board with minimal scattering material. The thicknesses and material budget of these boards are similar to those of the cylindrical support structures for the scintillating fiber tracking system proposed for the SDC[2] with a total radiation length $\sim 0.5\%$ per superlayer. Three such superlayers formed the fiber tracking system for this test.

2.4 Clear Waveguides

The scintillating fibers were mated to 6 m long undoped fibers (waveguides) of the same diameter to pipe the light to the VLPCs for detection of the light. Simple butt joints, using mineral oil to wet the cut and polished surfaces, were used. Alignment was accomplished by using mated aluminum connectors which held the fibers in position. Care was taken to ensure that the radius of curvature of the clear waveguides was $\geq$ 10 cm in order to avoid damage to the waveguides. The scintillating fiber and waveguides were produced commercially[9].

2.5 Visible Light Photon Counters

The photodetectors used in this beam test are Visible Light Photon Counters (VLPCs), a variant of the Solid State Photomultiplier (SSPM). The original HMC/HISTE-I devices[10] had quantum efficiencies of about 85% at $\lambda = 565$ nm. Because of the high quantum efficiency of the HMC/HISTE-I devices for electromagnetic radiation in the long wavelength region ($1 \leq \lambda \leq 28$ μm), there have been restrictions[11] on their use. A program initiated by the authors focussed on working with Rockwell International Science Center to develop versions with quantum efficiency $\leq$ 2% for $\lambda \geq 1$ μm which would not have restrictions. Tests using 16 channels of HISTE-I VLPCs[12] and 32 channels of HISTE-II VLPCs[13] have been reported. The VLPCs used in this test are from the lot known as HISTE III. A new lot, HISTE-IV, has recently been produced with approximately 1 mm diameter round pixels and improved quantum efficiency.

The properties of the HISTE-III VLPCs used in this beam test are summarized in Table 1.

Quantum efficiency	55%
Operating temperature	7 K
Bias voltage	8.5 V
Gain	$\sim 20,000$

Table 1. Properties of the HISTE-III VLPCs.

VLPCs must operate at a temperature between 6 K and 8 K, so a liquid helium cryostat is required for their operation. The VLPC quantum efficiency is a slow function of temperature. At lower temperatures electronic noise is reduced and the gain is increased because a higher bias voltage can be used. In our test four 8-pixel VLPC arrays were mounted on an oxygen-free copper mounting plate, and the ends of clear waveguides were carefully aligned with the pixels. As shown in Figure 4, this mounting plate was then placed inside a copper can, and the whole assembly was inserted into a very loosely fitting copper pipe in a 5-liter liquid helium cryostat. Although a resistive heater and controller

were available, it was simpler and just as stable to control the temperature by moving the cassette assembly up or down in the cryostat. At a fixed position, the temperature of the VLPC assembly was stable to better than ±0.1 K. The 5-liter cryostat was able to maintain a stable operating temperature for 24 to 36 hours before refilling was required.

To test the system operating range, a bias voltage scan of all the VLPCs was carried out simultaneously. The number of tracks per trigger was measured as a function of bias voltage. The results of this scan are shown in Figure 5. The system clearly achieved a plateau at about 8.5 V. Because of the possibility of damage to the VLPCs, bias voltages greater than 8.6 V were not attempted.

A total of 96 scintillating fibers was instumented for this test. Due to microbonding problems for some VLPCs, 17 of the 96 channels were not active in the experiment. This microbonding problem has been eliminated in HISTE-IV by placing the microbonding pad away from the active VLPC pixel.

2.6 Data acquisition and trigger system

A diagram showing the data path is shown in Figure 6. The analog data from each of the 96 VLPC channels were first amplified by VTX preamplifiers[14] placed on the stem of the VLPC cassette. A second stage of amplification was provided by an amplifier-shaper-discriminator (ASD) module. The ASD generated analog output as well as binary hit output for analog values above a certain threshold. The binary hit data were provided to a prototype trigger card, which searched preprogrammed roads for hits in the superlayers to identify stiff tracks. The ASD had a single discrimination level for a set of 48 channels. This resulted in only two discrimination settings for all 96 channels. The coincidence of scintillation counters S1, S2, and S3 were used as the actual trigger for the data taken. Data from the prototype trigger system were recorded and compared to the data that passed through the analog data path.

The prototype trigger card used combinatorial logic to convert the binary hit data into track segments corresponding to a stiff track passing through a superlayer. This was done by including all segments defined by a line from hits on the doublet on the upstream side of the superlayer to hits on the downstream side, which were within a range of angle that corresponded to a high p_t track. The candidate stiff track segments in each superlayer were compared using combinatorial logic to select the ones which had a curvature corresponding to a stiff track. Some typical events which the digital trigger identified as having a stiff track are shown in Figure 7. The output of the trigger card was four bits of data which denoted whether a stiff track occurred and the charge of the particle generating that track. The prototype card was developed using discrete programmable array logic devices (PALs); the trigger logic will be eventually implemented using application specific integrated circuits (ASICs). There was one PAL device for the segment finder and one for the segment linker. Since there was no magnetic field at the fiber superlayers to provide momentum selection, there was no curvature in the tracks. In the beam test this device was, therefore, essentially a track trigger, not a high p_t trigger as would be used in a magnetic spectrometer. To test the operation of this device for high rate conditions similar to SSC, a test transmitter was

designed which could operate the card at 50 MHz. Data corresponding to candidate stiff tracks were loaded into the memory of the test transmitter, and presented to the trigger card in the same fashion as it would come from the fibers. This test operation of the trigger card at the SSC data rate using input data to simulate tracks in the SDC central tracker was very successful and all candidate high p_t tracks gave triggers.

The analog data were digitized using two LeCroy 1885F fastbus analog-to-digital converters. This data were then transmitted to a personal computer (PC) through a LeCroy 1821 fastbus crate controller. The binary data were collected by the trigger card housed in a VXI crate. The four bits of trigger data, binary hit data, and track segments were transferred from the trigger card to the PC through a VME to PC interface. All of the analog and digital data were temporarily stored on disk and later transferred to an 8 mm tape drive and to other computers over an ethernet connection. The PC provided an on-line display of the pulse height distribution for a user selected channel as well as a map of the hit channels for the most recent event. The maximum collection rate for the system was 300 to 400 events per second.

The integrated charge distribution for a typical VLPC channel is shown in Figure 8. The threshold used for determining whether an ADC channel had a hit or not was determined channel by channel by setting it equal to the average ADC count value plus 1.7 times the width of the pedestal. The distribution of thresholds for the active VLPC channels is shown in Figure 9. The threshold settings are clustered in two peaks, the largest at about 280 ADC counts and the other at about 300 counts. A channel-by-channel examination revealed a systematic upward shift in threshold every fourth channel, which corresponds to the peak at about 300 counts. The cause of this shift is unknown. If all channels are considered, the distribution has a root mean square deviation of about 20 counts, indicating a a small channel to channel gain variation.

2.7 Tracking algorithm

Finding tracks in the fibers was accomplished by using an algorithm that tested the χ^2 per degree of freedom on candidate tracks. To find a track, a straight line was drawn through a pair of hit fibers in superlayers one and three. The hit fibers within a tracking window ($\sim \pm 1$ fiber diameter) of this straight line were found. A best fit line was then drawn through this set of candidate hits. The hit fibers within a new tracking window ($\sim \pm 1/2$ fiber diameter) of this fit line were found, and singlet and doublet coordinates were calculated and a new fit was made.

The fibers within the tracking window ($\sim \pm 1/2$ fiber diameter) of this second fit line were then determined. The algorithm continued this iteration until the found hits were the same for two steps of the iteration. These hits were designated as a possible track and the χ^2/degree of freedom was found. In order for this track to have been used in the analysis, there must have been at least six hit fibers on it and at least one hit fiber from every superlayer. The algorithm continued drawing best fit lines and finding the hits within the tracking windows of the fit lines until all the pairs of hits on the first and third superlayers were used.

2.8 Spatial resolution

To find the spatial resolution of a doublet layer of scintillating fibers, a straight line was drawn through a pair of hit fibers in the first and sixth ribbon doublets. The hit fibers within 1/2 fiber diameter of this straight line were found. In Figure 10 the spatial distribution of hits relative to the straight line described above are shown for various doublet layers of scintillating fibers. These histograms show narrow peaks, which are characteristic of the digital tracking nature of a scintillating fiber or a silicon strip tracking system. The position assigned to a single hit in a doublet is the center position of the hit fiber. For double hits (a hit in one layer plus an adjacent hit in the second layer of the doublet) the position is halfway between the centers of the two hit fibers. The observed root mean square deviations are 207, 178, 200, and 208 μm for doublet layers 2, 3, 4, and 5 respectively. These measurements contain uncertainties from the determination of the track coordinates from the first and sixth doublets as well as that from the doublet layer itself. For the outer doublet layers 2 and 5 the true doublet resolution can be unfolded by simply taking the root mean square deviation divided by $\sqrt{2}$. This yields a spatial resolution of 146 μm. For the inner doublet layers 3 and 4 the true doublet resolutions are found by taking the root mean square deviations of the observed distributions divided by $\sqrt{3/2}$. This gives a resolution of 145 μm for doublet layer 3 and 163 μm for doublet layer 4. Thus, the average spatial resolution is $\sim$ 150 μm, which is within $\sim$ 20% of the expected value of (850 μm)/($2\sqrt{12}$) = 123 μm given by equation (1).

2.9 Photostatistics

A Monte Carlo simulation of the fiber tracker was developed to unfold the average number of photoelectrons produced by a minimum ionizing particle. The geometry used in the simulation was that obtained from the calibration of the superlayers found using charged particle tracks. The fiber diameter, the cladding thickness, and the spacing between fibers were also simulated.

Seventeen of the 96 fibers were not active in the experiment, due to breakage of wire bonds to the VLPC bonding pads[15] and scratches inadvertently made during cassette construction. Some of the bad channels were identified by plotting pedestals and removing channels with extreme pedestal widths. Dead channels were identified by studying of the fiber hit histogram. Those channels which did not participate in the tracking were removed. From these analyses, a list of bad channels was created and those bad channels were excluded in the Monte Carlo in order to simulate the system appropriately.

Noise was determined in the data by finding the number of fibers that fired but were not associated with a track. Noise in the Monte Carlo was simulated by assigning a small probability for a fiber to randomly fire (approximately 15 kHz). This probability was adjusted until the fibers not associated with a track in the Monte Carlo and the actual data were in agreement. The noise occupancy of a VPLC channel from this adjustment was about 3%, which is in agreement with the examination of extra hits not associated with tracks in the tracking analysis.

The input to the Monte Carlo was the number of photoelectrons produced by a particle as it traversed the center of the fiber. This peak value was scaled by the amount of material the track traversed as it passed through the fiber. The number of photoelectrons produced by a minimum ionizing charged particle was determined by scaling the Monte Carlo input according to how far the track was from the center of the fiber.

Using Poisson statistics, the probability for a fiber to fire was determined. Tracks were defined by the same method as in the track finding algorithm and the number of fibers that participated in a track was found. In the Monte Carlo the number of fibers that participated in a track was plotted as a function of photoelectrons. The average number of photoelectrons produced in the system was then calculated by comparing the number of fibers on a track in the data to the number of fibers on a track in the Monte Carlo. The photoelectron yield was determined by the Monte Carlo distribution which gave the lowest χ^2 when compared to the real data. The average photoelectron yield was found by multiplying the peak photoelectron yield input to the Monte Carlo by $\pi/4$, the average weight for a circular fiber.

The number of photoelectrons produced by a minimum ionizing particle is shown as a function of the distance from the joint between the scintillating fiber and clear waveguide joint in Figure 11. The data can be fitted with a straight line with a slope of -0.146 photoelectrons per meter. Near the the joint between the scintillating fiber and clear waveguide joint (1.7 ± 0.1) photoelectrons were detected, while at the farthest point, 4.3 m from the joint, (1.2 ± 0.1) photoelectrons were detected.

3. Conclusions

This beam test was an important milestone in the understanding of the performance of a scintillating fiber charged particle tracking system. It demonstrated the ability of a scintillating fiber system to track charged particles with a spatial resolution $\sigma \sim 150$ μm, which is close to the theoretical limit given by equation (1), and the ability to operate a large number of channels under identical bias voltage and temperature settings. It also resulted in the successful operation of a prototype Level 1 trigger using scintillating fibers.

At the time of the beam test the optimum components necessary for an SSC fiber tracker were unavailable. A number of improvements have become available through our recent research and development efforts. They are listed below and summarized in Table 2.

1. Larger VLPC pixels ($\sim$ 1 mm diameter) are available. This diameter can be compared to the 900 μm square pixels used in this test. These larger pixels allow an increase in fiber diameter which will give more path length for charged particle energy loss by ionization. The larger fiber diameter also reduces the number of reflections when light propagates in a fiber. These two effects improve the photoelectron yield by a factor ≥ 1.3.
2. The improved VLPCs (HISTE-IV) have quantum efficiencies of $\sim$ 70% compared to the 55% quantum efficiency for the HISTE-III VLPCs used in the test beam run. This improves the photoelectron yield by a another factor of 1.3.

3. The optimal concentration of the 3-HF secondary fluor depends on the length and diameter of the scintillating fiber. For the 4.3 m length used in the beam test, the optimal concentration is 0.15% instead of the 0.1% used for the beam test. Measurements by the authors show that this optimumization improves the photoelectron yield by a factor of 1.2.
4. Recent measurements on double-clad scintillating fibers show 1.7 times more light yield than the single-clad fibers used in the beam test. The additional outer cladding is a fluorinated acrylic.
5. It is estimated that the fiber-to-fiber coupling efficiency was about 65%; recently finer polishing and improved optical connectors have achieved 95% efficiency for a single fiber. It is estimated that 85% for a mass termination connector is achievable, giving an improvement in photoelectron yield of 1.3.

With these improvements this beam test establishes the viability of a scintillating fiber charged particle tracking system capable of operating at the SSC and LHC. A new test is being prepared to verify the complete system now that all of the optimum components are available.

Component	Change	Improvement factor
VLPC	HISTE-III → HISTE IV	1.3
Scintillation dye	concentration optimization	1.2
Fiber core diameter	835 μm → 965 μm	1.3
Cladding	single → double	1.7
Optical coupling	polishing and connector design	1.3
	Overall	4.5

Table 2. Improvement factors in photon yield unavailable at time of the beam test.

4. Acknowledgments

The Scintillating Fiber Group wishes to thank the technical staffs of their home institutions and the Brookhaven National Laboratory staff for their hospitality. We appreciate the work of J. C. Cooper, M. L. Cooper, K. Chua, and D. Vandergriff in preparing the scintillating fiber ribbons and mounting them accurately on the carbon fiber composition boards. This work has been supported in part by the U.S. Department of Energy, the National Science Foundation, and the Texas National Research Laboratory Commission.

REFERENCES

1. The Visible Light Photon Counter is a variant of the Solid State Photomultiplier (SSPM), both of which have been developed by of the Rockwell International Science Center, Inc., Anaheim, CA 92803.
2. Solenoidal Detector Collaboration, *Technical Design Report*, SSCL-SR-1215 (1992).
3. Subsequently it has been determined that 0.15% by weight is a better concentration level.
4. A. D. Bross and A. Pla-Dalmau, Conference Record of the 1991 IEEE Nuclear Science Symposium (Santa Fe, NM, Nov. 5-8, 1991), pp. 1493–1497.
5. This water-based glue was obtained from Bicron Corporation, 12345 Kinsman Road, Newbury, OH, and consists of a 70% urethane and 30% acrylic mixture.
6. P.-T. Chou and M. L. Martinez, Rad. Phys. Chem. 41, 373 (1993).
7. The boards were manufactured by the Composite Structures Division of Hercules Aerospace Co., Migna, UT 84044.
8. Rohacell is a lightweight polymethacrylimide foam manufactured by Cryo Industries, Orange, CT 06477
9. Kuraray International Corporation, 200 Park Avenue, NY, was the source of our scintillating fibers. Bicron Corporation, 12345 Kinsman Road, Newbury, OH, has also supplied us with scintillating fibers and clear waveguides.
10. HISTE stands for HIgh-rate Scintillating fiber Tracking Experiment. HMC stands for HISTE Mask Checkout.
11. The use of HMC/HISTE-I devices is restricted by the U.S. Department of Defense under the International Traffic in Arms Regulation (ITAR).
12. M. Atac et al., Nucl. and Meth. **A320**, 155 (1992).
13. B. Abbott et al., Nucl. Inst. and Meth. **A327**, 319–327 (1993).
14. The VTX amplifier is a preamplifier designed by R. J. Yarema et al. for the Vertex Time Projection Chamber at the Colliding Dedector at Fermilab.
15. The microbonding problem has been eliminated in the HISTE-IV devices by placing microbonding pads away from the active VLPC pixels.

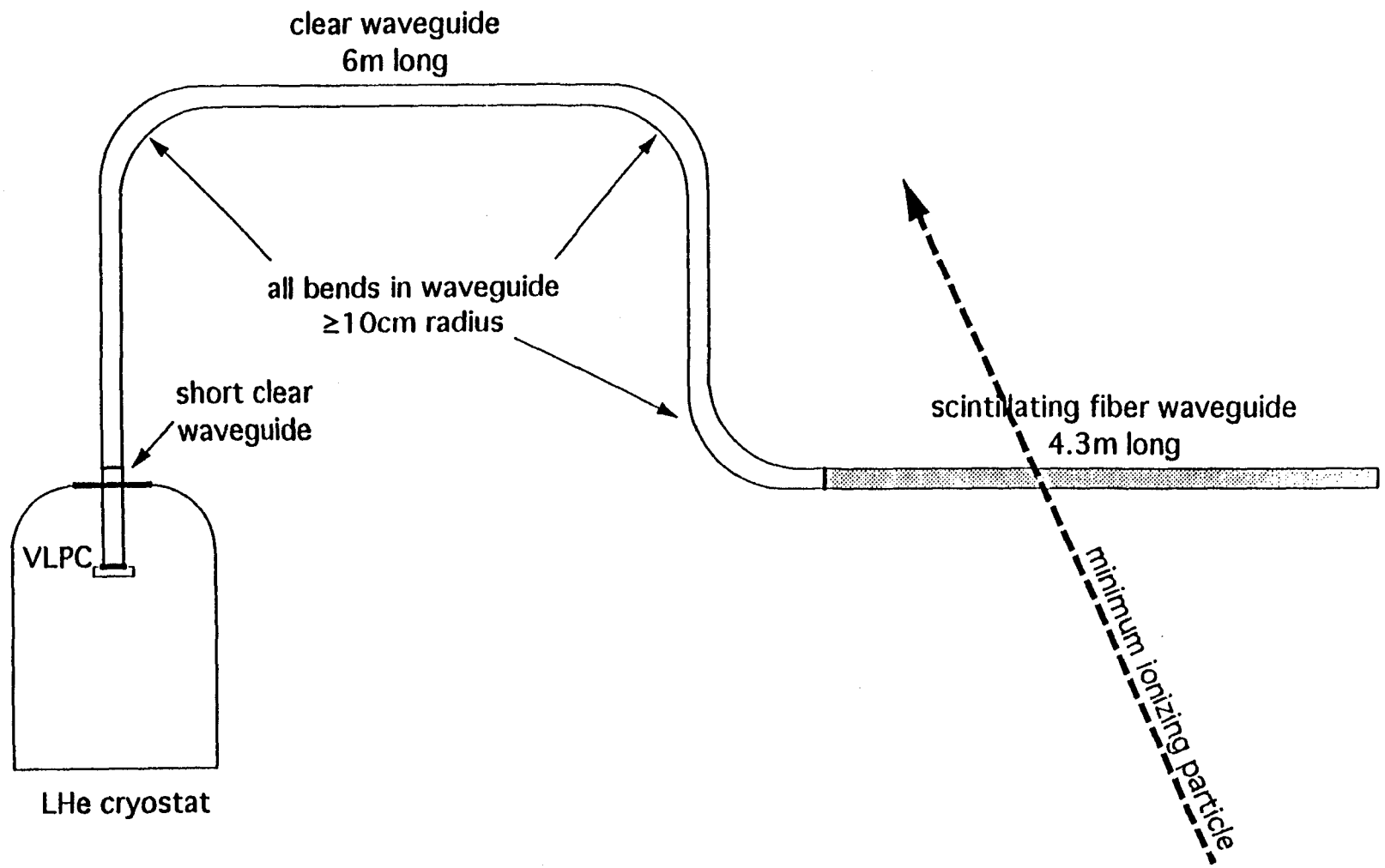

1. Schematic diagram of a single channel of a scintillating fiber charged particle tracking system.

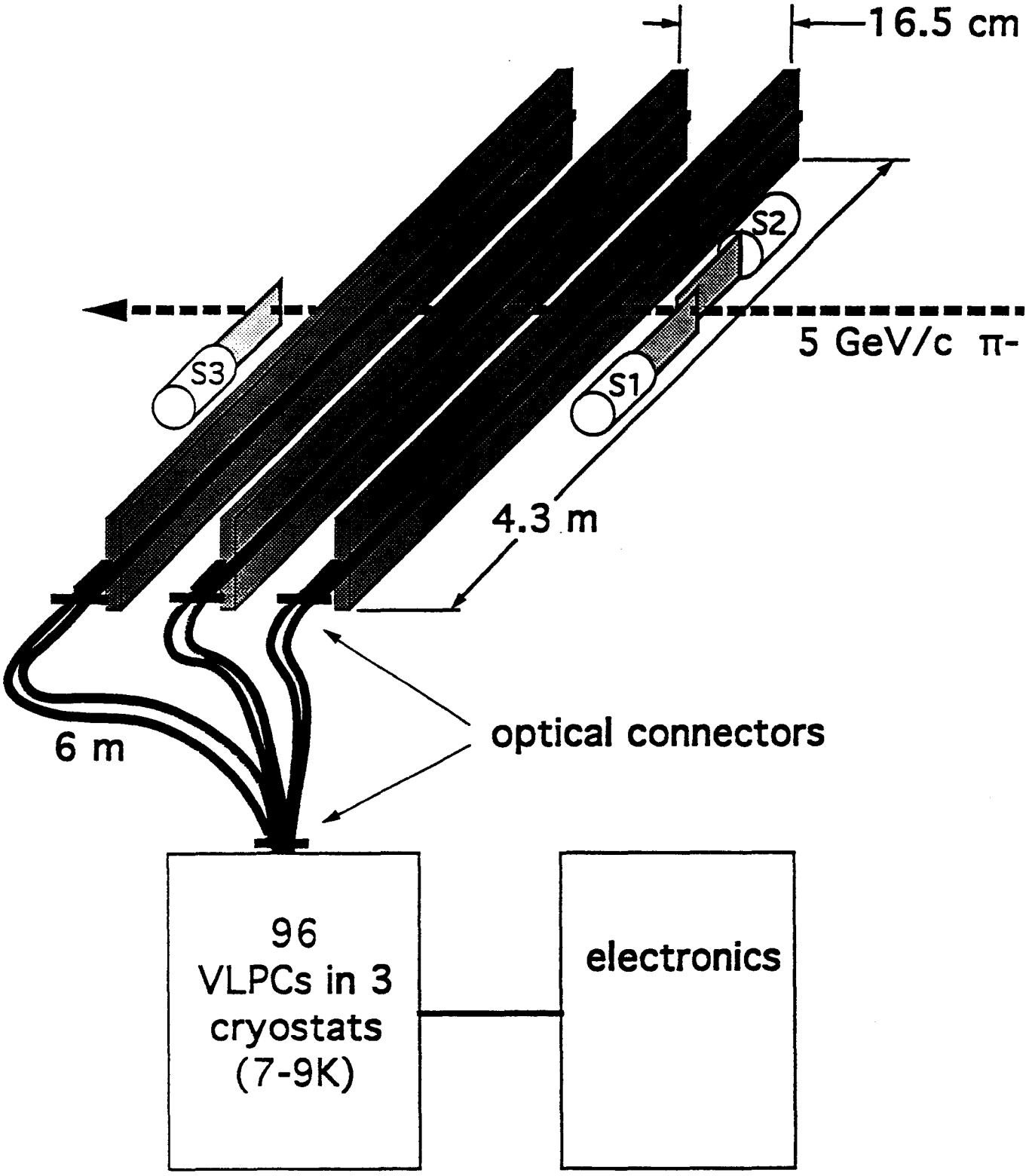

2. Layout of the scintillating fiber charged particle tracking system in a 5 GeV/c π^- test beam at Brookhaven National Laboratory.

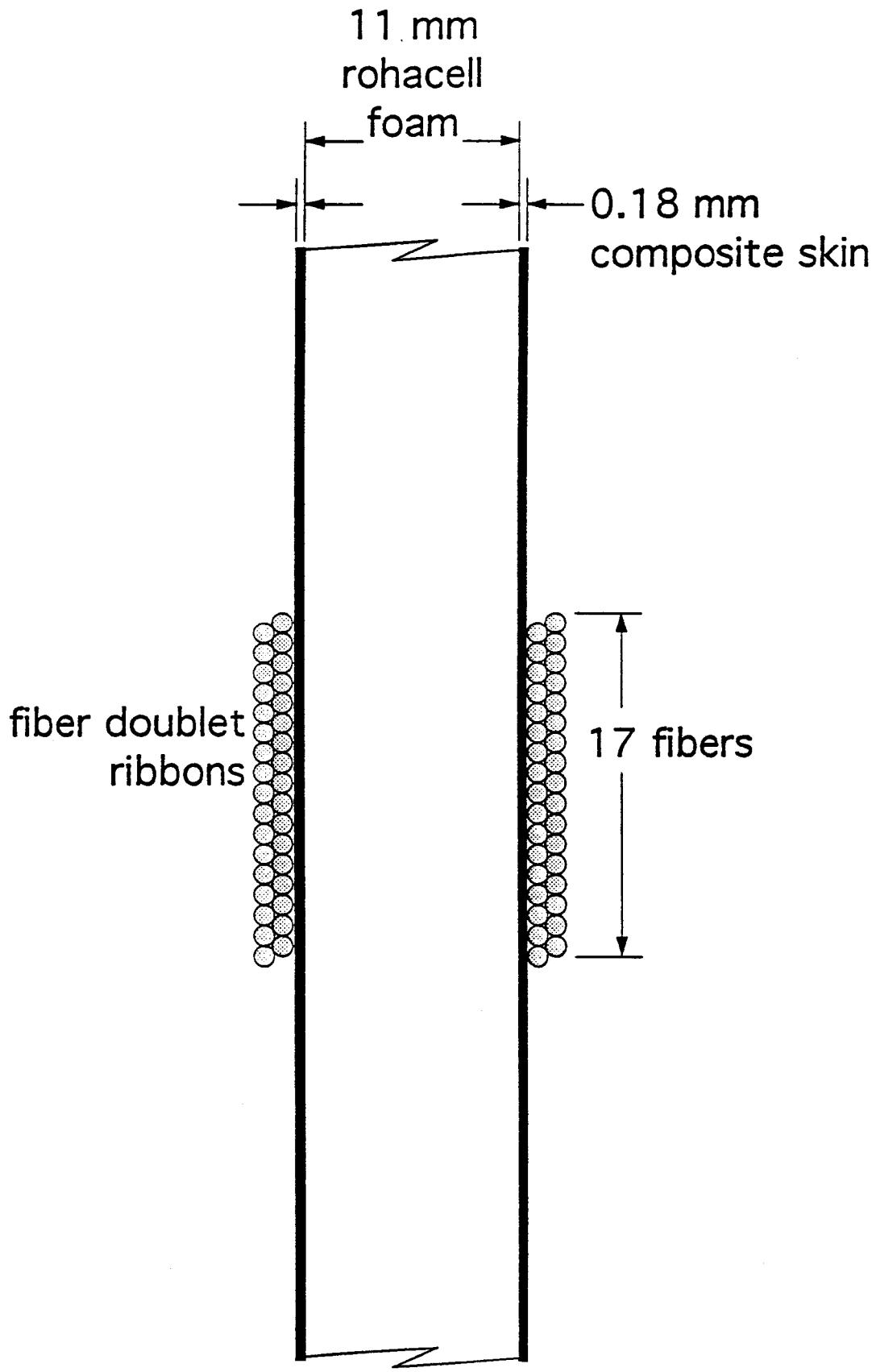

3. Superlayer of scintillating fibers made by gluing double-layered ribbons on each side of a composite carbon fiber-epoxy board.

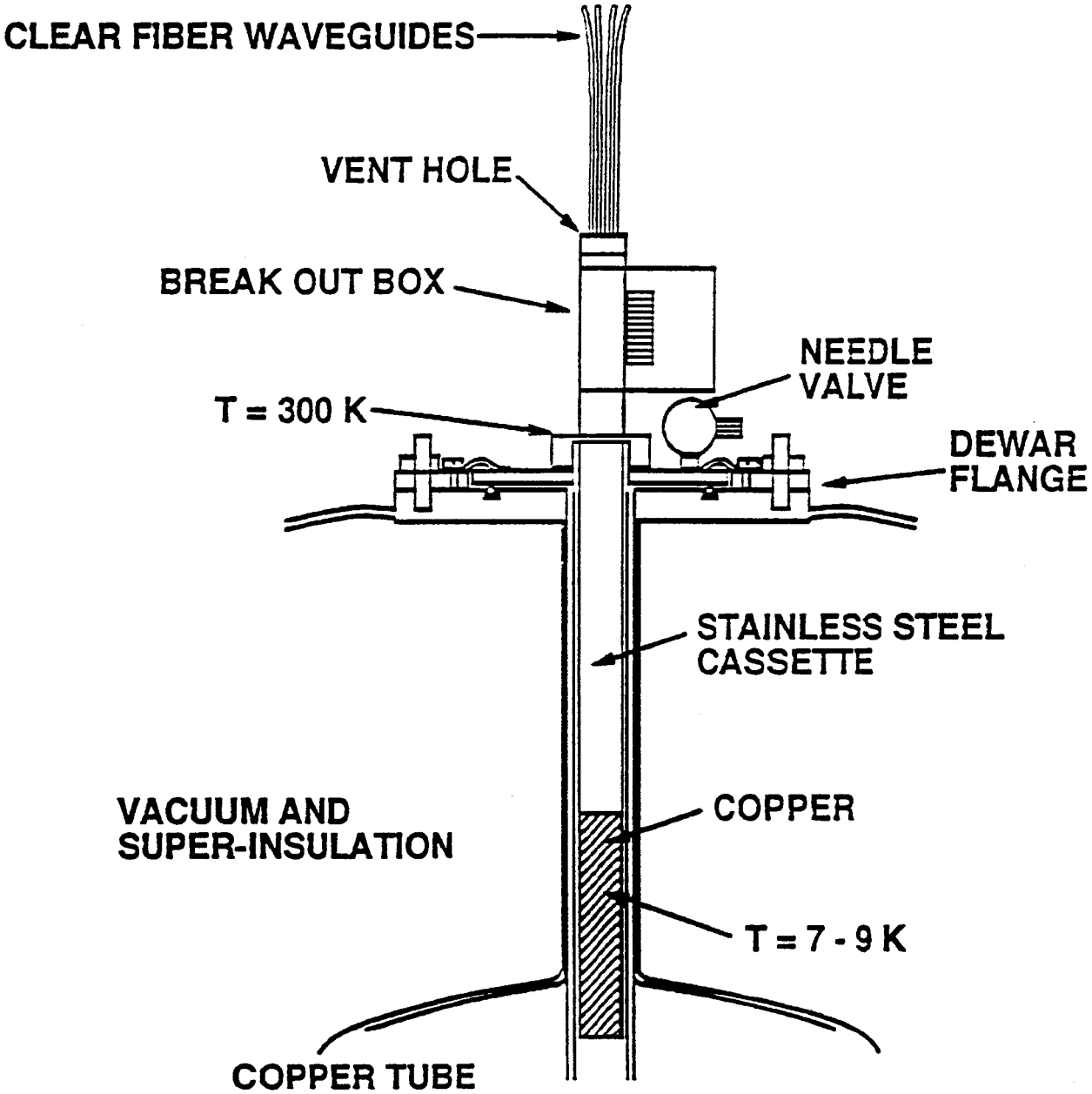

4. Diagram of a 32-channel VLPC cassette in a cryostat.

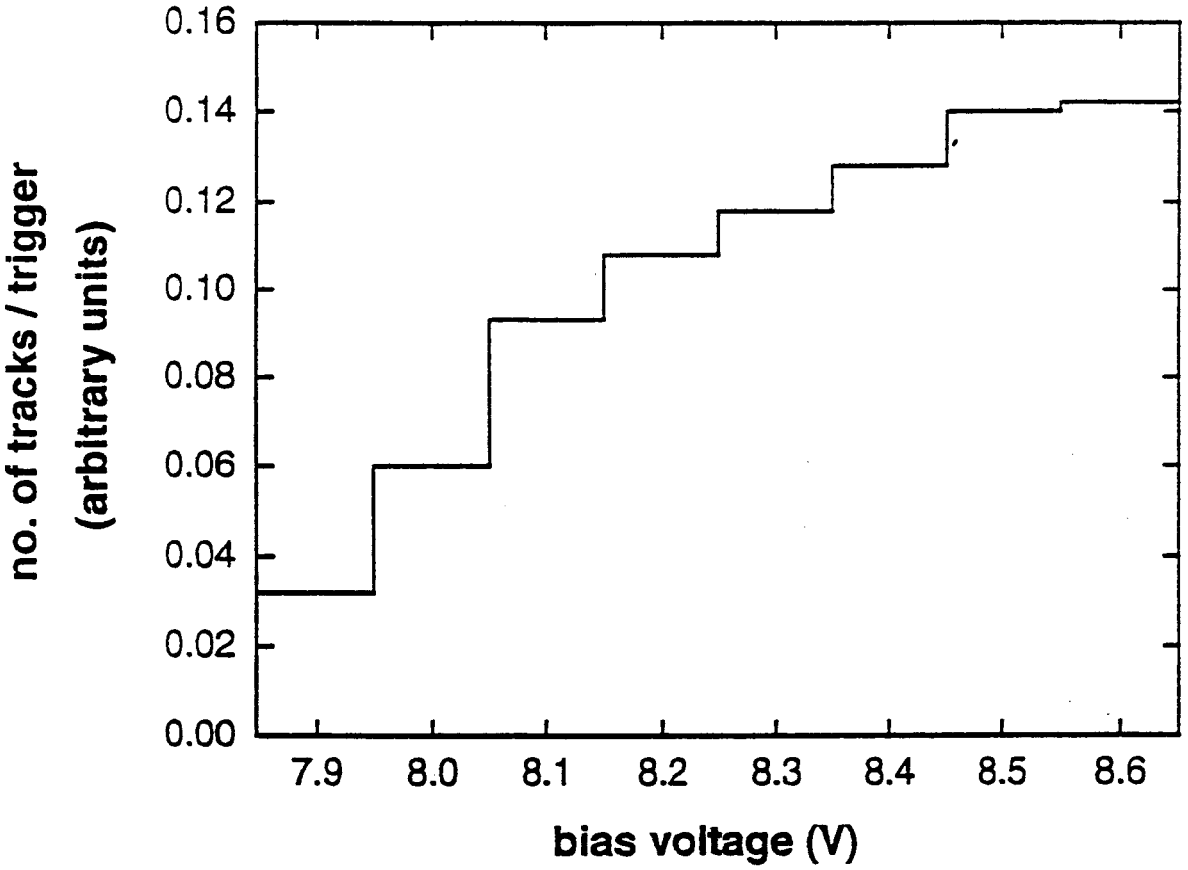

5. Number of tracks as a function of VLPC bias voltage.

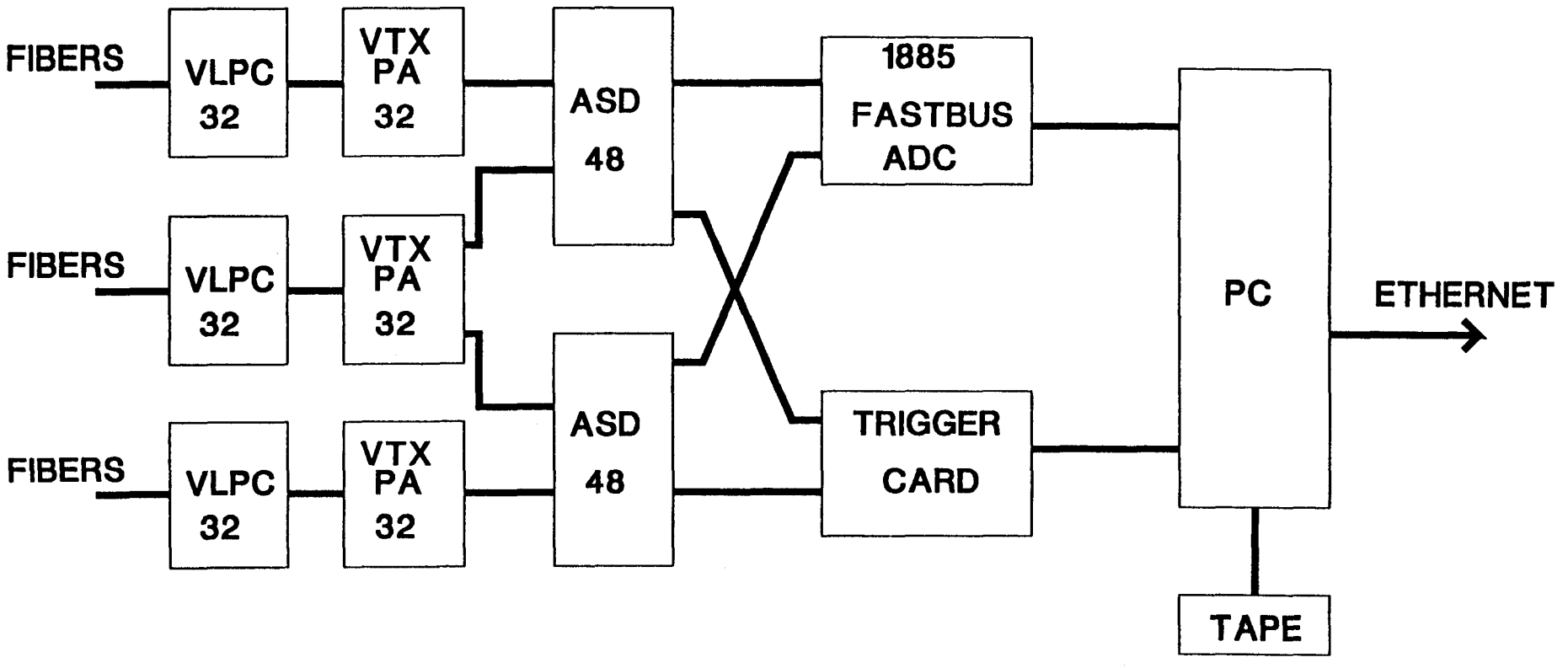

6. Schematic diagram of the data path. The analog data from the VLPCs were amplified in two stages by VTX preamplifiers (VTX PA) and then by an amplifier-shaper-discriminator (ASD) module. The ASD module generated both analog output, which went to LeCroy Model 1885 analog-to-digital converters (1885 fastbus ADC), and binary hit output, which went to a prototype trigger card. Both the ADCs and the trigger card were read by a personal computer (PC) and their data were written to tape and passed to remote sites by ethernet.

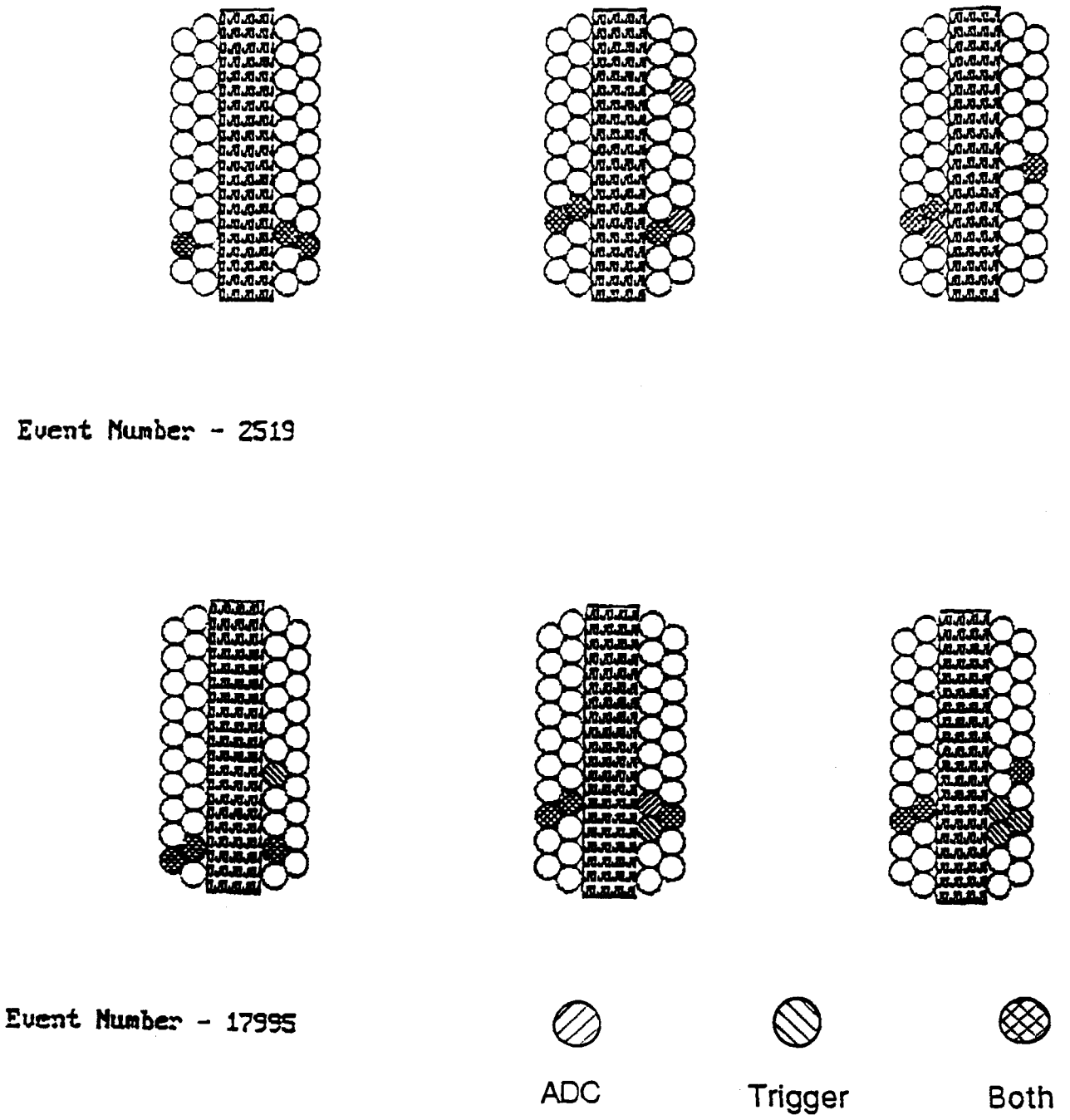

7. Two typical events showing hits according to the ADC system, the prototype trigger system, and both systems. These events were identified by the prototype trigger system as having a straight track.

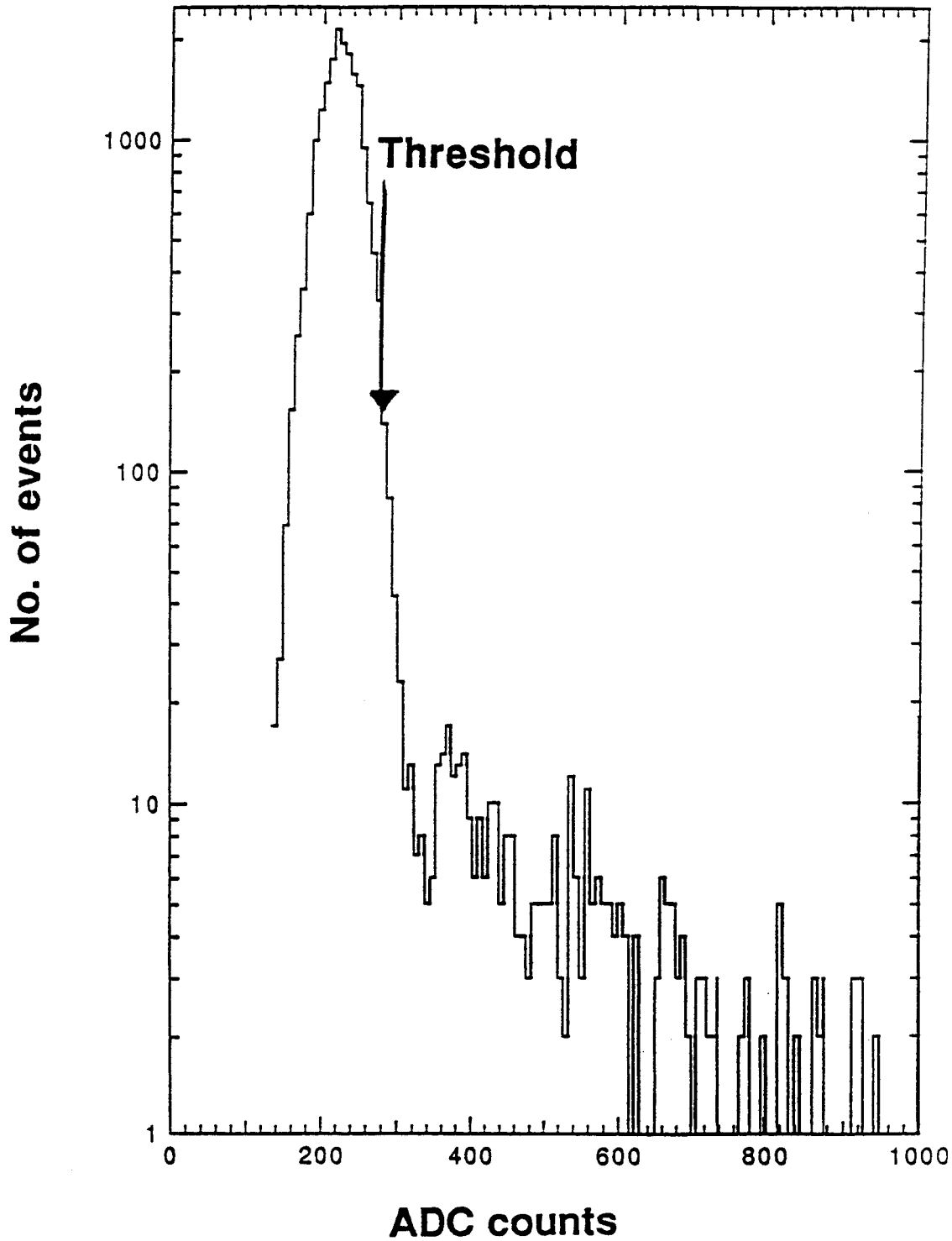

8. Integrated charge distribution for a typical VLPC channel in units of ADC counts, where 1 ADC count is about 0.25 pC. The arrow indicates where the threshold setting for a hit or no hit decision.

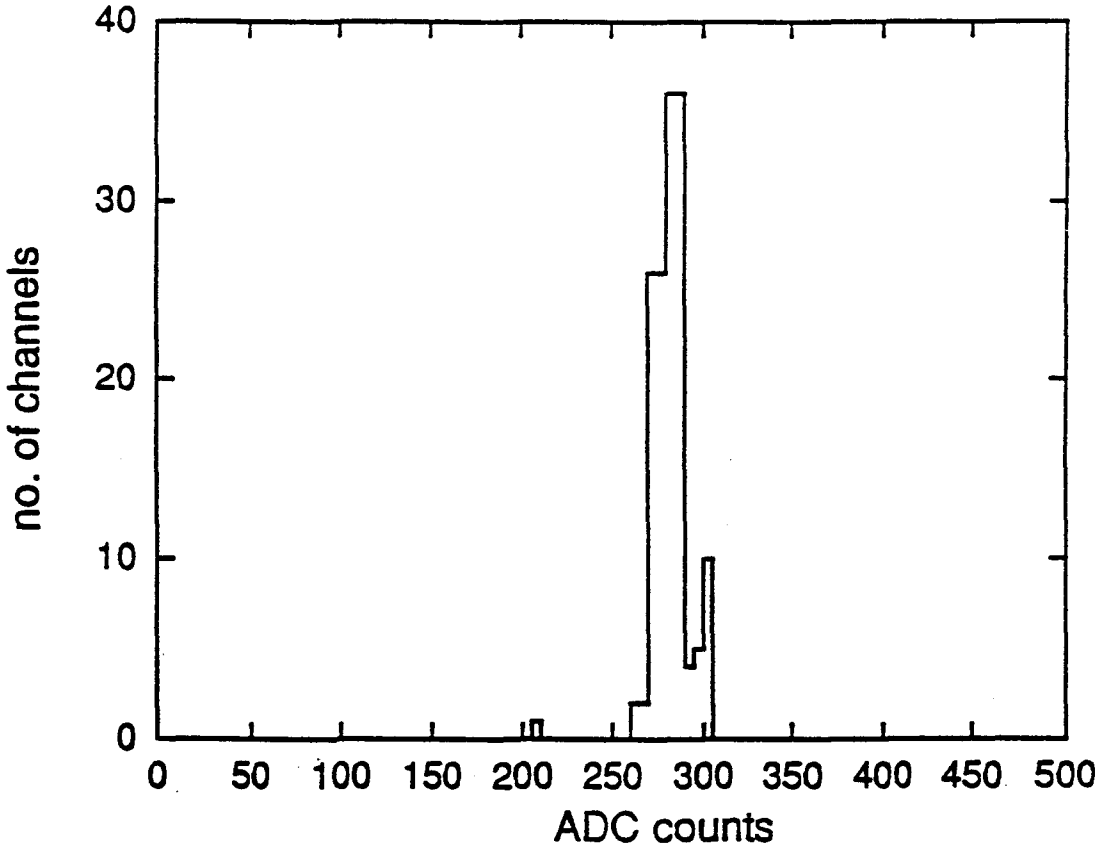

9. Distribution of ADC thresholds for active VLPC channels. The threshold for an individual channel was determined by taking the average count value plus 1.7 times the width of the pedestal. The smaller peak at about 300 ADC counts is due to a systematic upward shift in threshold every fourth ADC channel.

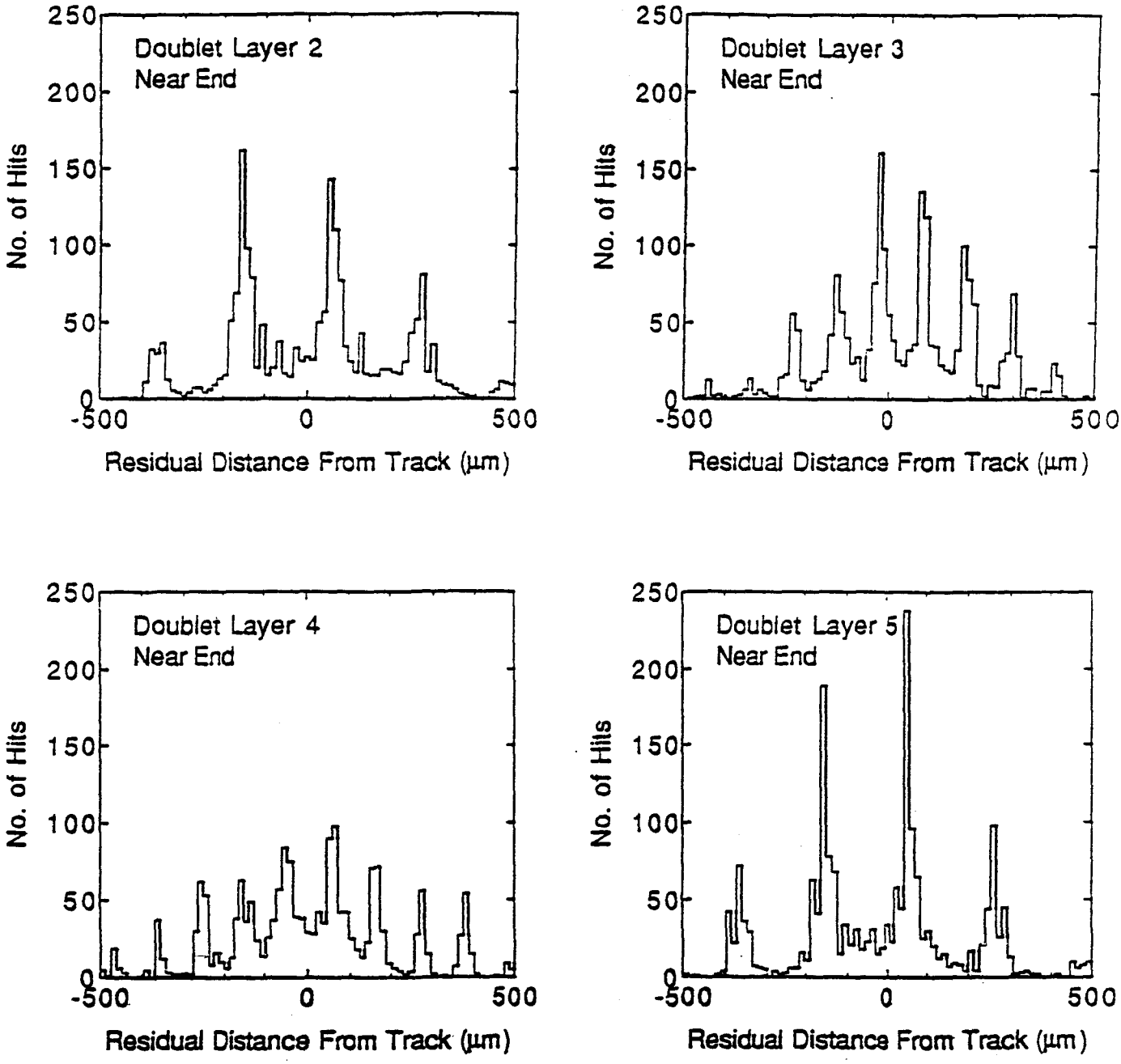

10. Spatial resolution of hits in the four inner doublet layers. The root mean square deviations are 207, 178, 200, and 208 μm for inner doublet layers 2, 3, 4, and 5, respectively. These deviations give scintillating fiber doublet resolutions of 146, 145, 163, and 146 μm for these doublet layers.

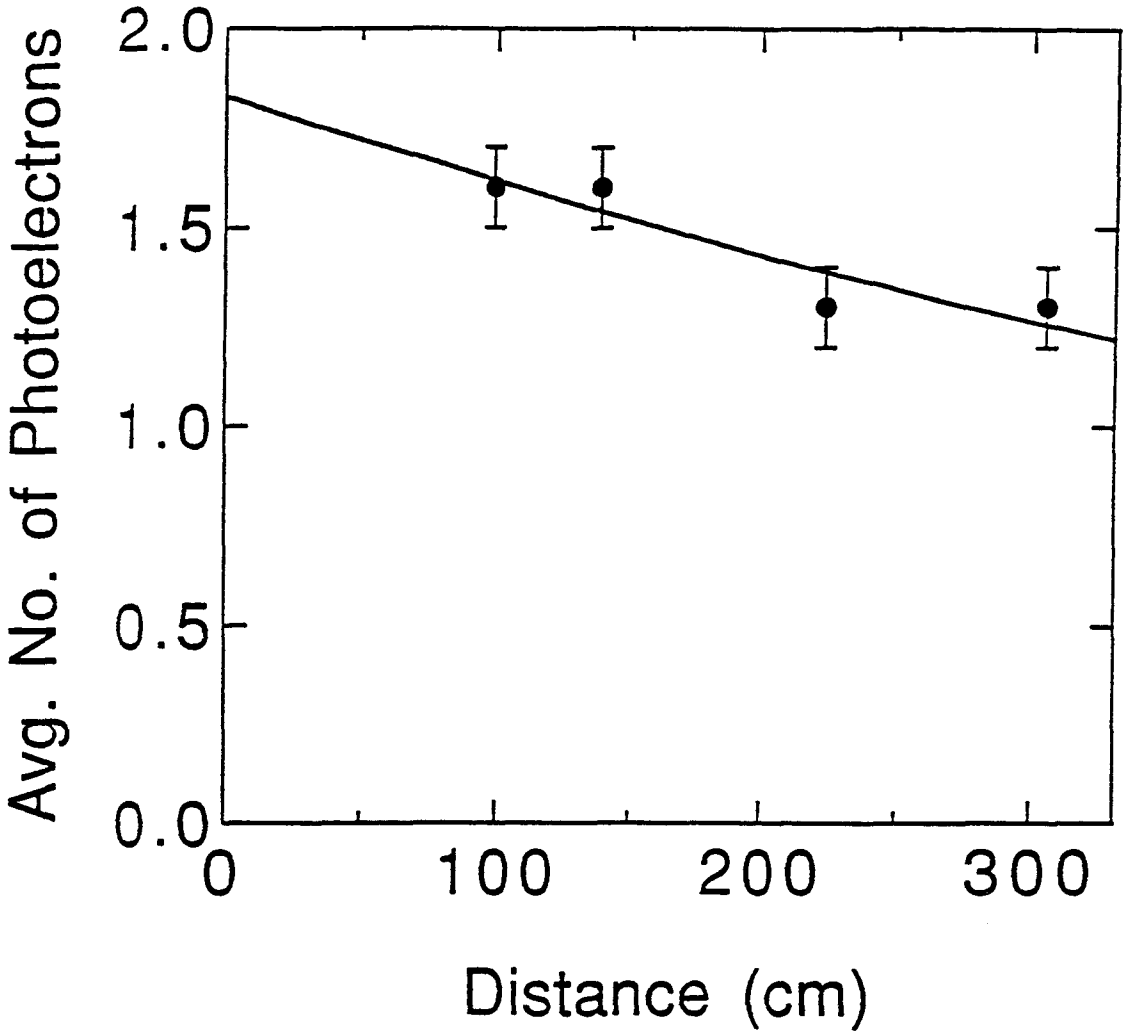

11. The number of photoelectrons produced by a minimum ionizing particle as a function of the distance from the joint between the scintillating fiber and clear waveguide joint.